

Comparative Inhibition Study of New Synthesised Pyridazine Derivatives Towards Mild Steel Corrosion in Hydrochloric Acid. Part-II : Thermodynamic Proprieties

B. Zerga¹, B. Hammouti², M. Ebn Touhami^{3,*}, R. Tourir³, M. Taleb¹, M. Sfaira¹, M. Bennajeh³, I. Forssal³

¹ Laboratoire d'Ingénierie des Matériaux, Modélisation et Environnement, Faculté des Sciences Dhar El Mahraz, BP 1796, 30000 Atlas, Fès – Morocco.

² LCAE-URAC18, Faculté des Sciences, Université Mohammed I^{er} B.P. 717, 60000 Oujda, Morocco.

³ Laboratoire d'Electrochimie, Corrosion et Environnement, Faculté des Sciences, BP 133, 14000 Kénitra – Morocco.

*E-mail: mebntouhami@yahoo.fr

Received: 10 November 2011 / Accepted: 12 December 2011 / Published: 1 January 2012

The corrosion rates in the presence of new synthesised pyridazine derivatives (P1, P2, P3 and P4) as a steel corrosion inhibitors in 1 M hydrochloric acid, were measured by the weight loss method, in the range of temperatures from 303 to 353 K. Results obtained revealed that the inhibition efficiency of these compounds decreases markedly with increasing temperature and its value reaches 48.5% at 353 K at 10⁻³M. The inhibition was assumed to occur via adsorption of the pyridazine molecules on metallic surface. Adsorption of inhibitor molecules on steel surface showed Langmuir adsorption isotherms fit in acidic media. The apparent activation energies (E_a), enthalpies (ΔH_a) and entropies of activation (ΔG_a) values provide evidence of the inhibitory effect of pyridazine derivatives. Furthermore, spontaneity, through equilibrium constant (K_{ads}) values and free energy value (ΔG_{ads}) of the adsorption process, shows a drastic decrease upon temperature increase in the presence of P1.

Keywords: Synthesised pyridazine derivatives; Adsorption process; Corrosion inhibition; Thermodynamic proprieties.

1. INTRODUCTION

Corrosion in mineral acids represents a terrible waste of both natural resources and money [1]. Among the best corrosion inhibitors that act as major adsorption centres are some organic compounds, containing functional electronegative groups and π -electron in triple or conjugated double bonds. These hetero-atoms, such as sulfur, phosphorus, nitrogen, and oxygen, together with heterocyclic or

conjugated aromatic, play significantly in inhibition process [2-6]. Furthermore, the most synthesised compounds are the nitrogen-heterocyclic compounds which are known to be excellent complex or chelate forming substances with metals of transition series. Their adsorption is generally explained by the formation of an adherent film on the metal surface [7-11].

The introduction of sulphur atom in heterocyclic compounds containing nitrogen has proved very good corrosion inhibition of metals in acidic solutions [12-14]. Their inhibitive power is related to the various active adsorption centres as cyclic rings or hetero-atoms. The higher inhibition efficiency of hetero-atoms as oxygen, nitrogen, phosphorus and sulphur should follow the sequence $O < N < S < P$ [14].

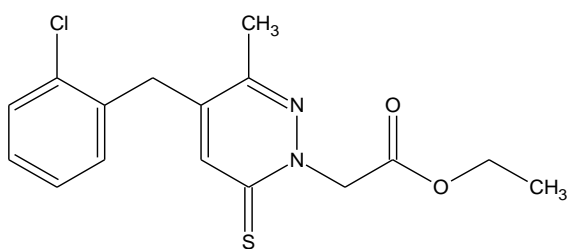
The choice of pyridazine compounds is based on their much known pharmaceutical application in the inhibition of aldose reductive and exhibiting antioxidant properties [15, 16] and the presence of two nitrogen and sulphur atoms in pyridazine ring with various substituents.

In the present work, we investigate the corrosion inhibition of mild steel in 1 M HCl by some newly synthesised pyridazine compounds at different temperature range. Kinetic and thermodynamic parameters were investigated to give deeper insight to the effect of inhibitor structure using weight loss measurements.

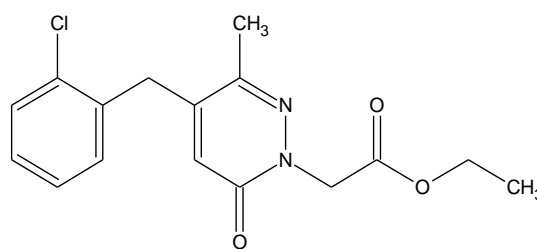
2. EXPERIMENTAL DETAILS

Prior to all measurements, the mild steel samples (0.21% C; 0.38% Si; 0.09% P; 0.01 %Al; 0.05% Mn; 0.05% S and the remainder iron) was used in the form of sheets with $2 \times 2 \times 0.05$ cm dimensions which were degreased with acetone, polished with different emery paper up to 1200 grade, dried, and weighed until used.

The aggressive solution (1 M HCl) was prepared by dilution of analytical grade 37% HCl with bidistilled water. Gravimetric measurements were carried out in a double walled glass cell equipped with a thermostat-cooling condenser. The solution volume was 100 cm^3 . The molecular formula of pyridazine derivatives is shown in Fig. 1.



P1 : ethyl [4-(2-chlorobenzyl)-3-methyl-6-thioxopyridazin-1(6H)-yl]acetate



P2 : ethyl [4-(2-chlorobenzyl)-3-methyl-6-oxopyridazin-1(6H)-yl]acetate

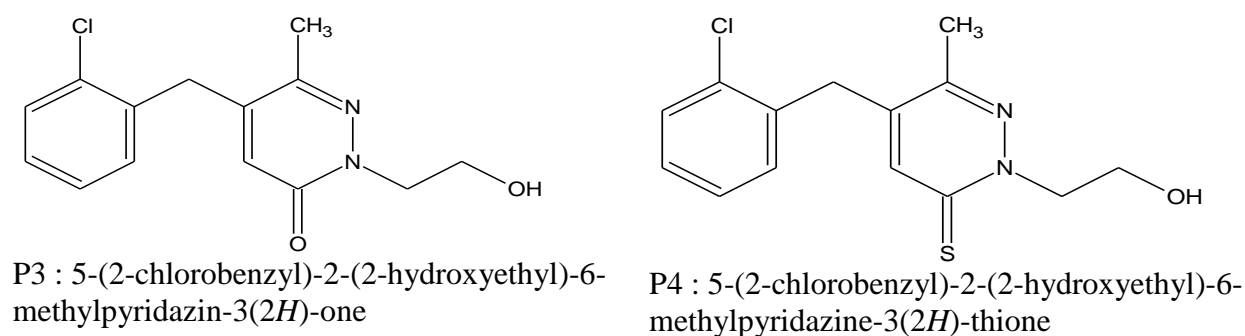


Figure 1. Chemical structure of new synthesised pyridazine derivatives.

3. RESULTS AND DISCUSSION

3.1. Effect of temperature

Table 1. Corrosion parameters obtained from weight loss measurements at various temperatures studied for mild steel in 1M HCl of P1, P2, P3 and P4 at 10^{-3} M.

Temperature (K)	Compounds	W_{corr} (mg/cm ² .h)	$IE_{\text{w}}\%$
313	1M HCl	1.30	–
	P1	0.1	92
	P2	0.19	85
	P3	0.24	82
	P4	0.20	85
323	1M HCl	3.47	–
	P1	0.58	83
	P2	0.76	78
	P3	0.92	74
	P4	0.72	79
333	1M HCl	6.72	–
	P1	1.69	75
	P2	2.35	65
	P3	2.73	59
	P4	2.40	64
343	1M HCl	10.8	–
	P1	3.60	67
	P2	5.18	52
	P3	5.54	49
	P4	5.0	54
353	1M HCl	19.20	–
	P1	10.20	47
	P2	10.77	44
	P3	11.67	39
	P4	11.13	42

To evaluate the adsorption of pyridazine derivatives and extract the activation parameters of corrosion processes of mild steel in acidic media, weight-loss measurements were used. The inhibition efficiency ($IE_w\%$) is calculated as follows:

$$IE_w\% = \left(1 - \frac{W_{corr}}{W_{corr}^0}\right) \times 100 \tag{1}$$

Where W_{corr} and W_{corr}^0 are the corrosion rates of mild steel in the absence and presence of the organic compounds, respectively.

Table 1 presents the corresponding data of mild steel immersed for 1h in corrosive solution containing $10^{-3}M$ of P1, P2, P3 and P4 separately at different range of temperature 303–353 K.

It is well-known that corrosion rate increases with the rise of temperature in acidic media for all inhibitors.

The variation of corrosion rate and inhibition efficiency with temperature for steel in 1 M HCl of pyridazine compounds at $10^{-3}M$ is shown in Fig. 2. It is note the decrease in the inhibition efficiency with increasing of temperature. It is well-known that the rise in temperature leads to an increase in corrosion rate with and without inhibitor.

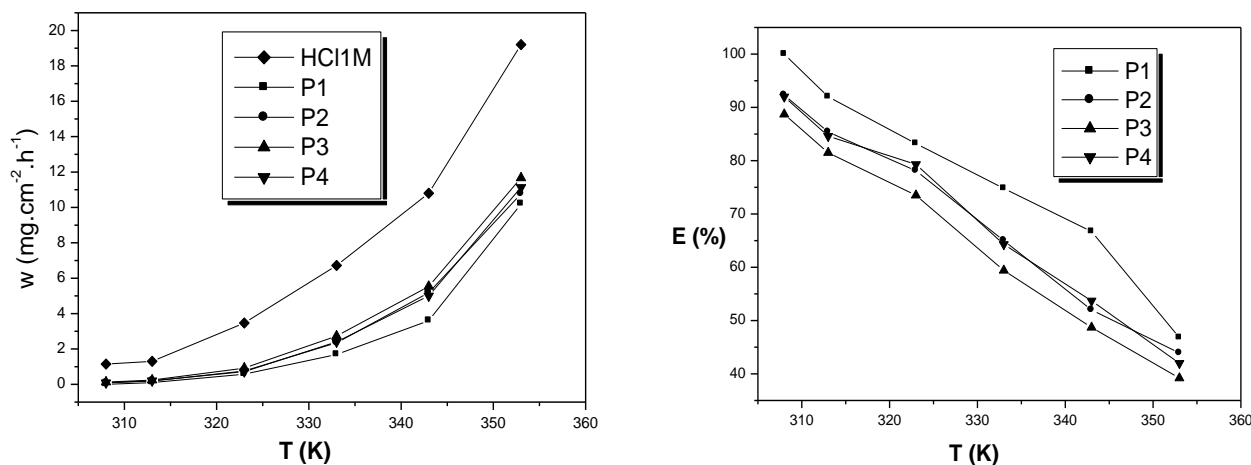


Figure 2. Variation of corrosion rate and inhibition efficiency with temperature for mild steel in 1 M HCl in the presence of $10^{-3}M$ of P1, P2, P3 and P4 separately

The effect of the temperature shows that the increase of corrosion rate is more pronounced with the rise of temperature for the blank solution. In the presence of inhibitors, W_{corr} is generally reduced and the inhibition efficiency ($IE_w\%$) depends on the temperature and decreases from 92 to 48 % when the temperature rises from 313 to 353 K at $10^{-3} M$ of P1. It is also notice that P1 has the best effectiveness. In the continuation of this work we made a detailed study for this product in order to determine the thermodynamics parameters and to explain the adsorption mechanism.

3.2. Study of ethyl [4-(2-chlorobenzyl)-3-methyl-6-thioxopyridazin-1(6H)-yl]acetate (P1)

3.2.1. Effect of immersion time

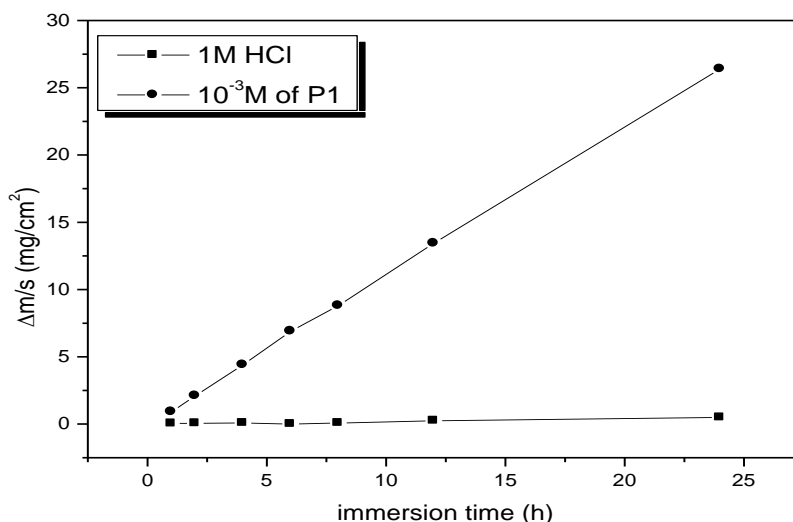


Figure 3. Weight loss versus immersion time of mild steel in 1 M HCl without and with 10⁻³ M of P1 at 303 K.

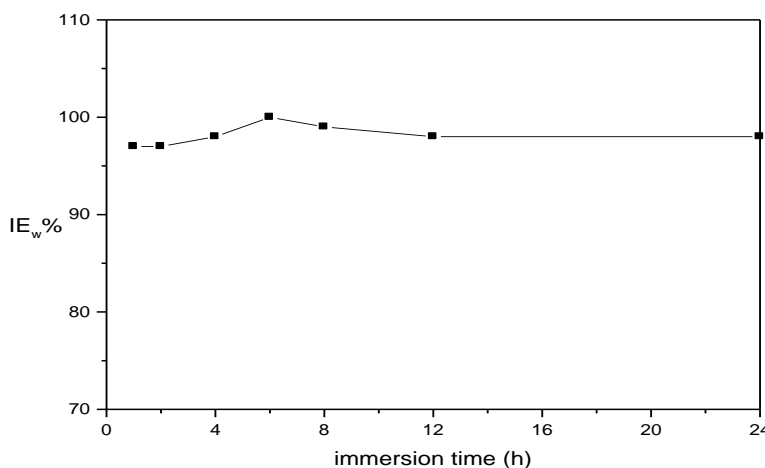


Figure 4. Variation of IE_w (%) versus immersion time of mild steel in 1 M HCl without and with 10⁻³ M of P1 at 303 K.

Fig.3 shows the effect of addition of P1 at 10⁻³M on the corrosion of mild steel in 1M HCl solution was studied by weight loss measurements at 303 K at various immersion periods.

The effect of increasing time on the weight loss of mild steel in uninhibited and inhibited acid solutions is shown in Fig. 3. It is obvious that the weight loss varied linearly with immersion period in plain acid and inhibited acid, showing the absence of insoluble product on the mild steel surface [17]. The curve obtained in the presence of the additive fall significantly below that of free acid. The

relatively large divergence of the plots indicates the increase of IE_w (%) with time as shown in Fig. 4. It is note that the inhibition efficiency attains 100% since 6 h to attain more than 98% at 24 h at 303 K. This result promises also its use even during a period.

3.2.1. Effect of temperature

Table 2. Influence of temperature on the corrosion rate and inhibition efficiency of mild steel in 1 M HCl at different concentrations of P1.

Temperature (K)	Concentrations (M)	W_{corr} (mg/cm ² .h)	IE_w %
313	0	1.30	–
	10^{-6}	0.67	49
	10^{-5}	0.57	56
	5×10^{-5}	0.465	64
	10^{-4}	0.325	75
	5×10^{-4}	0.178	86
	10^{-3}	0.1	92
323	0	3.47	–
	10^{-6}	1.94	44
	10^{-5}	1.73	50
	5×10^{-5}	1.62	53
	10^{-4}	1.25	64
	5×10^{-4}	0.86	75
	10^{-3}	0.58	83
333	0	6.72	–
	10^{-6}	4.16	38
	10^{-5}	3.89	42
	5×10^{-5}	3.14	53
	10^{-4}	2.54	62
	5×10^{-4}	1.93	71
	10^{-3}	1.69	75
343	0	10.8	–
	10^{-6}	7.65	29
	10^{-5}	7.44	31
	5×10^{-5}	6.48	40
	10^{-4}	5.29	51
	5×10^{-4}	3.90	64
	10^{-3}	3.60	67
353	0	19.20	–
	10^{-6}	15.55	19
	10^{-5}	14.94	22
	5×10^{-5}	13.50	29
	10^{-4}	12.48	35
	5×10^{-4}	10.90	43
	10^{-3}	10.20	47

Table 2 presents the values of corrosion rate of mild steel at different concentrations of P1 were determined by weight loss measurement at various temperatures (303-353 K) and the corresponding inhibition efficiencies. It is well-known that corrosion rate increases with the rise of temperature in acidic media. At each temperature, the inhibition corrosion increases with inhibitor concentration. But at a given inhibitor concentration, the inhibitory effect ceases more and more to jump from 92% at 303 K to 47% at 353 K. Apparently, the results obtained postulate that the inhibitor function through adsorption on the metal surface by the blocking the active sites to form a screen onto the mild steel surface from acidic solution. As the temperature increases, we notice the desorption rate manifests parallel to that of adsorption [18]; the surface becomes less protected and then the inhibitor gradually loss its effectiveness.

3.2.3. Kinetic parameters of activation

The influence of temperature on the kinetic process of corrosion in free acid and in the presence of adsorbed inhibitor leads to get more information on the electrochemical behaviour of metallic materials in aggressive media.

To calculate activation thermodynamic parameters at different concentrations of P1 such as activation energy E_a , entropy ΔS° and enthalpy ΔH° of activation, Arrhenius Eq. (2) and its alternative formulation called transition state Eq. (3) were used:

$$W = K \exp\left(-\frac{E_a}{RT}\right) \quad (2)$$

$$W = \frac{RT}{Nh} \exp\left(\frac{\Delta S_a^\circ}{R}\right) \exp\left(-\frac{\Delta H_a^\circ}{RT}\right) \quad (3)$$

T is the absolute temperature, K is a constant and R is the universal gas constant, h is plank's constant, N is Avogadro's number.

The activation energy E_a is calculated from the slope of the plots of $\text{Log}(W_{\text{corr}})$ vs. $1/T$ (Fig.5). Plots of $\text{Log}(W_{\text{corr}}/T)$ vs. $1/T$ give a straight line with a slope of $\Delta H^\circ/R$ and an intercept of $(\text{Log}(R/Nh) + \Delta S^\circ/R)$ as shown in Fig. 6. From this relation the values of ΔH° and ΔS° can be calculated. The calculated parameters at different concentrations of the inhibitor are collected in Table 3.

The activation energy increases in presence of the inhibitor. Generally, the inhibitive additives cause a rise in activation energy value when compared to the blank solution. The change of the values of the apparent activation energies may be explained by the modification of the mechanism of the corrosion process in the presence of adsorbed inhibitor molecules [19] and could be often interpreted as an indication for the formation of an adsorptive film by a physical (electrostatic) mechanism [15,16].

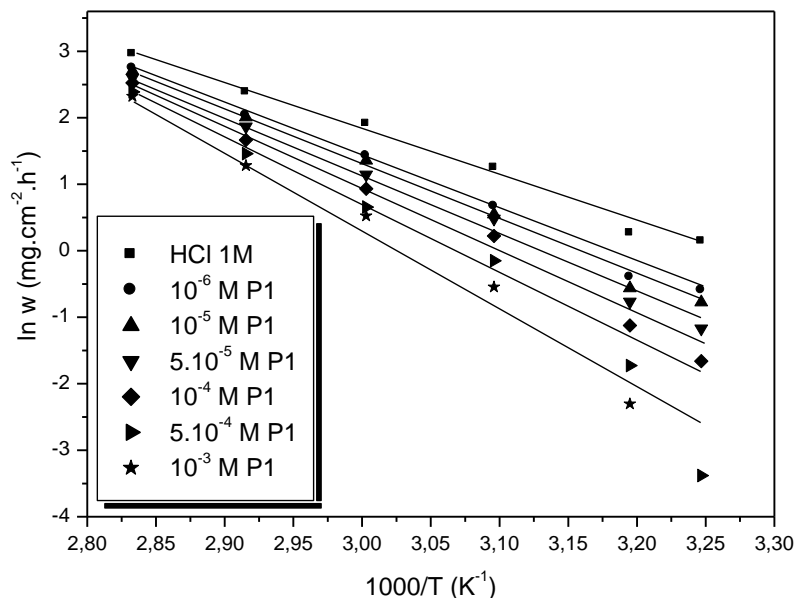


Figure 5. Arrhenius plots of mild steel in 1 M HCl at different concentrations of P1.

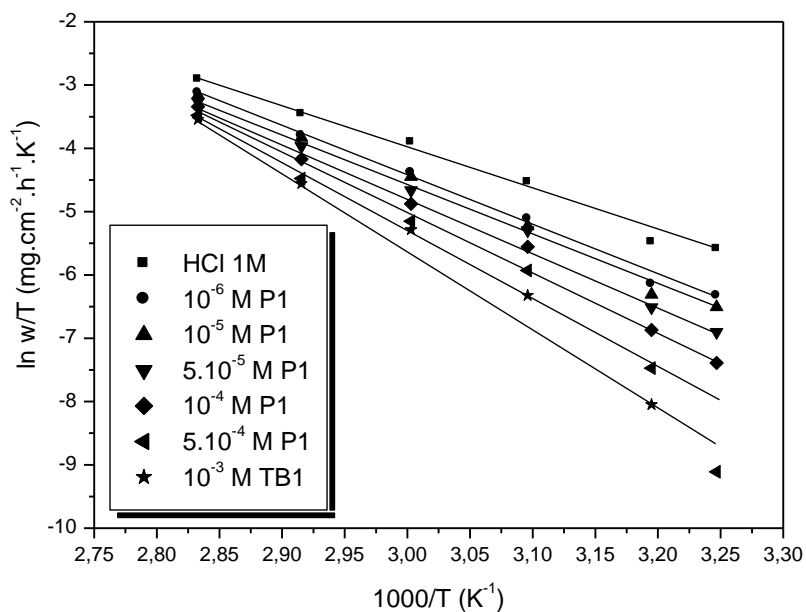


Figure 6. The relationship between $\ln(W/T)$ and $1/T$ for mild steel at different concentrations of P1.

Inspection of the kinetic data obtained in Table 3 shows that all parameters of corrosion process increases with the inhibitor concentration. Literature postulates that the positive sign of the enthalpy (ΔH_a°) is an endothermic nature of the copper dissolution process. The entropy of activation ΔS_a° in the absence of inhibitors is positive and this value increases positively with the P1 concentration. The

increase of ΔS_a° implies that an increase in disordering takes place on going from reactants to the activated complex [20].

In our case the values of ΔH° mean that the dissolution reaction is an endothermic process and that the dissolution of steel is difficult [21]. Also, the entropy ΔS° increases negatively with the presence of the inhibitor than the non-inhibited one. This reflects the formation of an ordered stable layer of inhibitor on the steel surface [22]. From the previous data, we can conclude that P1 is an effective inhibitor.

Table 3. Activation parameters of the dissolution reaction of mild steel in 1 M HCl in the absence and presence different concentration of P1

Concentration (M)	E_a (kJ.mol ⁻¹)	ΔH^0 (kJ.mol ⁻¹)	ΔS^0 (J.mol ⁻¹ .K ⁻¹)
1M HCl	58.71	55.97	-62.94
10 ⁻⁶	68.93	66.19	-35.98
10 ⁻⁵	72.11	69.39	-27.12
5×10 ⁻⁵	76.05	73.30	-16.56
10 ⁻⁴	83.03	80.34	2.58
5×10 ⁻⁴	106.58	103.92	69.64
10 ⁻³	156.33	153.59	214.57

3.2.4. Adsorption isotherm

The elevated temperature had an adverse effect on adsorption process, where inter- and intramolecular forces such as, electrostatic bond, coordinative bond, and even weaker interactions such as, π - π stacking interactions were weakened, loosened, and eventually decomposed. For this, it is widely acknowledged that adsorption isotherms provide useful insights into the mechanism of corrosion inhibition. In order to obtain the isotherm type model, one supposes that P1 acts via a simple adsorption mode. Thus, the apparent corrosion rate of the inhibited mild steel electrode is proportional to the ratio of the surface covered θ and that not covered (1- θ) by the inhibitor molecules.

The surface coverage, θ , was calculated according to the following equation:

$$\theta = \frac{W_{\text{corr}} - W_{\text{corr/inh}}}{W_{\text{corr}}} \quad (4)$$

Surface coverage values (θ) for the inhibitor were obtained from the weight loss measurements for various concentrations at different temperatures (303–343 K), as shown in Table 4. It is necessary to determine empirically which adsorption isotherm fits best to the surface coverage data in order to use the corrosion rate measurements to calculate the thermodynamic parameters pertaining to inhibitor adsorption.

Careful investigation performed for Temkin [23, 24], Langmuir [25], Frumkin [26] and Freundlich [27] isotherms (5)–(8) would show the most fitting isotherm with maximum regression coefficients, R^2 , using the following relationships:

$$\text{Temkin isotherm} \quad \exp(f \cdot \theta) = k_{ads} C \quad (5)$$

$$\text{Langmuir isotherm} \quad \theta / (1 - \theta) = k_{ads} C \quad (6)$$

$$\text{Frumkin isotherm} \quad \theta / (1 - \theta) \cdot \exp(-2f \cdot \theta) = k_{ads} C \quad (7)$$

$$\text{and Freundlich isotherm} \quad \theta = k_{ads} C \quad (8)$$

where k_{ads} is the equilibrium constant of the adsorption process, C the inhibitor concentration and f the heterogeneous factor of metal surface. The most fitting best fitted straight line is obtained for the plot of C_{inh}/θ versus C_{inh} with slopes around unity. The correlation coefficient (R^2) was used to choose the isotherm that best fit experimental data (Table 4). This suggests that the adsorption of P1 on the metal surface obeyed to the Langmuir's adsorption isotherm (Fig. 7). Equilibrium constant (K_{ads}) of adsorption process determined using (9) could be further used to determine free energy of adsorption as follows:

$$\Delta_{ads} G^\circ = -RT \ln(55.55 K_{ads}) \quad (9)$$

where 55.5 is the molar concentration of water, R is the universal gas constant, and T is the thermodynamic temperature. Table 4 summarizes the equilibrium constant and free energy of adsorption values in presence and absence of P1.

The negative values of standard free energy of adsorption ΔG°_{ads} ensure the spontaneity of adsorption process [28,29] and stability of the adsorbed layer on the steel surface. It is show that the calculated ΔG°_{ads} values, is ranging from about -40.27 to -36.29 kJ mol^{-1} , indicating, therefore, that the adsorption mechanism of the P1 on mild steel surface in 1 M HCl solution as typical of chemisorption. The possible mechanisms for chemisorption can be attributed to the donation π -electron by the aromatic rings, the nonbinding electron pair of two nitrogen and sulphur in pyridazine group, and the presence the ester group containing two oxygen atoms. Moreover, the chemisorption can be favoured by the P1 planarity [30].

The corrosion inhibition of P1 for mild steel may be well explained by using a thermodynamic model, so, the heat, the free energy and the entropy of adsorption are calculated to elucidate the phenomenon for the inhibition action of P1 (Table 4). According to the Van't Hoff equation [31]:

$$\ln(K) = -\frac{\Delta H^\circ_{ads}}{RT} + \text{Constant} \quad (10)$$

Where ΔH°_{ads} and K are the adsorption heat and adsorptive equilibrium constant, respectively.

The adsorption heat may be obtained from the linear regression between $\ln(K)$ and $1/T$ shown in Fig. 8. $\Delta S^\circ_{\text{ads}}$ can be deduced from the thermodynamic basic equation:

$$\Delta G^\circ_{\text{ads}} = \Delta H^\circ_{\text{ads}} - T\Delta S^\circ_{\text{ads}} \tag{11}$$

The negative values of $\Delta H^\circ_{\text{ads}}$ mean that the dissolution process is an exothermic phenomenon [32]. It assumed that an exothermic process is attributed to either physical or chemical adsorption but endothermic process corresponds solely to chemisorption. In an exothermic process, physisorption is distinguished from chemisorption by considering the absolute value of a physisorption process is lower than 40 kJ mol^{-1} while the adsorption heat of a chemisorption process approaches 100 kJ mol^{-1} [33]. In this study; the standard adsorption heat $-66.80 \text{ kJ.mol}^{-1}$ postulates that a chemical adsorption is more favoured. The negative values of $\Delta S^\circ_{\text{ads}}$ is generally explained an ordered of adsorbed molecules of inhibitor with the progress in the adsorption onto the mild steel surface [34].

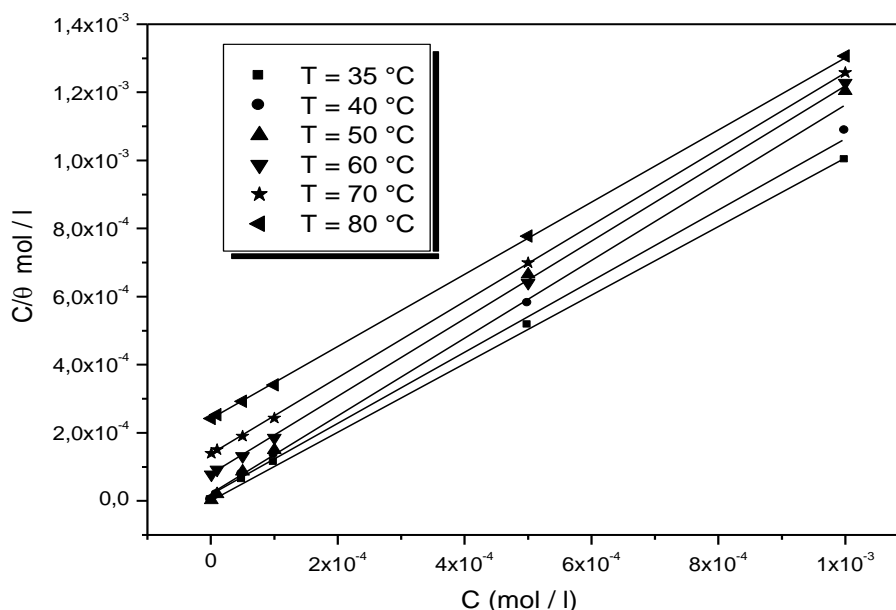


Figure 7. The relationship between C / θ and C of P1 at various temperatures.

Table 4. Thermodynamic parameters of adsorption of P1 on the mild steel surface at different temperatures

Temperature (K)	R ²	Slope	K	$\Delta G^\circ_{\text{ads}}$ (kJ.mol ⁻¹)	$\Delta H^\circ_{\text{ads}}$ (kJ.mol ⁻¹)	$\Delta S^\circ_{\text{ads}}$ (J.mol ⁻¹ K ⁻¹)
308	0.9999	0.9972	120586	-40.27	-66.68	-86.65
313	0.9999	1.08	60200	-39.12		
323	0.9999	1.2	37707	-39.10		
333	0.9999	1.14	13444	-37.47		
343	1	1.12	7375	-36.88		
353	1	1.06	4184	-36.29		

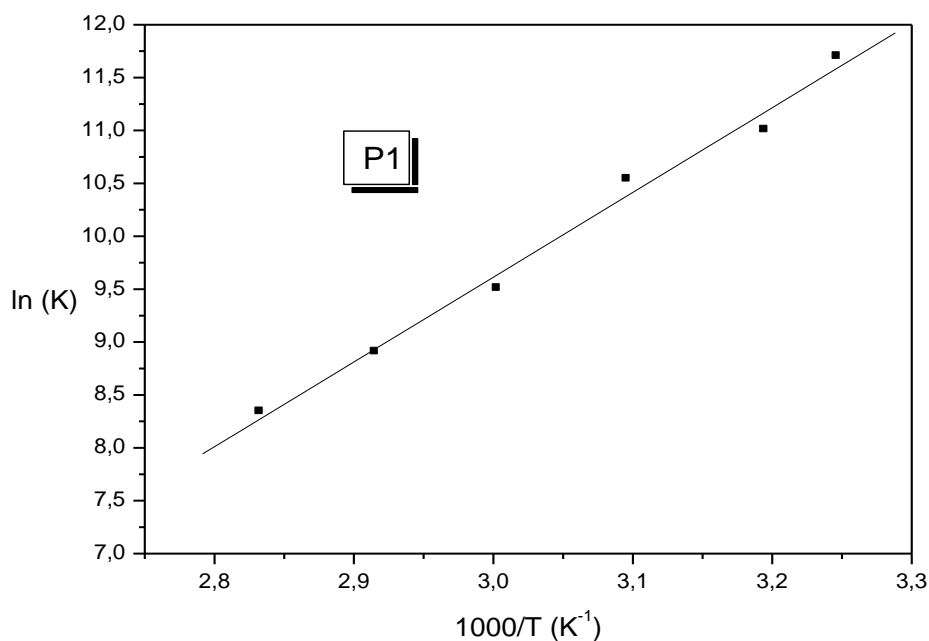


Figure 8. Vant'Hoff plot for the mild steel/P1/1M HCl system

4. CONCLUSION

Results obtained show that pyridazine derivatives tested are the efficient inhibitors.

- Inhibition efficiency increases with the increase of concentration and immersion time to attain 100% at 10^{-3} M for P1.
- Increase of temperature leads in a decrease of inhibition efficiency of all pyridazine and an increase of the activation corrosion energy.
- The most fitting isotherms in the adsorption of P1 at surface of mild steel acidic media were Langmuir isotherms and the negative value of $\Delta G_{\text{ads}}^{\circ}$ is a sign of spontaneous adsorption on the metal surface.
- In the presence of inhibitor, the inhibitory effect of P1 on mild steel was clarified using the apparent activation energy values (E_a); similarly, apparent entropy of activation showed that at larger inhibitor concentration solvent entropy increase in 1M HCl. At elevated temperatures, sudden spontaneity declines down, detected through equilibrium constant (K_{ads}) values and free energy value (ΔG_{ads}) due to weakening and decomposition of inter- and intramolecular interactions.

References

1. R. Javaherdashti, *Anti-Corros. Meth. Mater.* 47 (2000) 30.
2. H. Ju, Z.-P. Kai, and Y. Li, *Corr. Sci.* (2008) 865–871.
3. G. Schmitt, *British Corrosion J.* (1984) 165–176..
4. P. J. Sykes, *British Corrosion J.*(1993) 175–183.

5. S. Kertit, J. Aride, A. Ben-Bachir, A. Sghiri, A. Elkholy and M. Etman, *J. Applied Electrochemistry* (1989) 83–89.
6. A.K.Maayta, Mohammad M. Fares, and Ali F. Al-Shawabkeh, *Int. J. Corr.* (2010) 1-9 .
7. N.K. Patel, *J. Electrochem. Soc. India* 21 (1971) 136.
8. K. Wippermann, J.W. Schultze, R. Kessel, J. Penninger, *Corros. Sci.* 32 (1991) 205.
9. A.Dafali, B. Hammouti, A. Aounti, R. Mokhlisse, S. Kertit, K. Elkacemi, *Ann. Chim. Sci. Mater.* 25 (2000) 437.
10. B. Abdelnabi, N. Khalil, A. Mohamed, *Surf. Technol.* 24 (1985) 383.
11. A.Dafali, B. Hammouti, S. Kertit, *J. Electrochem. Soc. India* 50 (2001) 62.
12. J.G.N. Thomas, in: 5th Eur. Symp. on Corros. Inhibitors 1980, Ann. Univ. Ferrara, Italy, 1981, p. 453.
13. P. Coudert, C. Rubat, E. Duroux, P. Bastide, J. Couquelet, P. Tronche, E. Albuissou, *Farmaco* 47 (1992) 37.
14. S. Moreau, P. Coudert, B. Lasserre, D. Vallee-Goyet, D. Gardette, C. Navarro-Delmas, A.P. Huu Chanh, V. Dossou-Gbete, J. Couquelet, *Prostaglandins Leukot. Essent. Fat. Acids* 56 (1997) 431.
15. M. Schorr, J. Yahalm, *Corros. Sci.* 12 (1972).
16. N.P. Clark, E. Jakson, M. Robinson, *Br. Corros. J.* 14 (1979) 33.
17. M. Bouklah, B. Hammouti, M. Lagrenée, F. Bentiss, *Corr. Sci.*, 48 (2006) 2831–2842
18. A.Zarrouk, I. Warad, B. Hammouti, A Dafali, S.S. Al-Deyab, N. Benchat, *Int. J. Electrochem. Sci.*, 5 (2010) 1516 – 1526.
19. O. Riggs, I. R. Hurd, M. Ray, *Corrosion.*, 23 (1967) 252
20. A.Abd-El-Nabey, E. Khamis, M. Sh. Ramadan, A. El-Gindy, *Corrosion.*, 52 (1996) 671
21. N.M. Guan, L. Xueming, L. Fei, *Mater. Chem. Phys.* 86 (2004) 59.
22. A.Yurt, A. Balaban, S.U. Kandemir, G. Bereket, B. Erk, *Mater. Chem. Phys.* 85 (2004) 420.
23. M. I. Tempkin, *Zhurnal Fizicheskoi Khimii*, vol. 15 (1941), p. 296.
24. A.K.Maayta and N. A. F. Al-Rawashdeh, *Corr. Sci.*, vol. 46, no. 5, (2004) 1129–1140,.
25. I.Langmuir, “The constitution and fundamental properties of solids and liquids. Part I. Solids,” *The Journal of the American Chemical Society*, vol. 38, no. 2,(1916) pp. 2221–2295,.
26. A.N. Frumkin, “Electrocapillary curve of higher aliphatic acids and the state equation of the surface layer,” *Zeitschrift für Physikalische Chemie*, vol. 116(1925), p. 466,.
27. B. Berge, K. Grijotheim, C. Krohn, R. Neumann, K Torkiep, *light Metals*, (edited by S. R. Leavitt) proceeding of 105th annual meeting (1976) 23.
28. M.A.Migahed, *Mater. Chem. Phy.* 93 (2005) 48.
29. J.Cruz, R.Martinez, J.Genesca, E.G.Ochoa, *J.Electroan. Chem.* 566 (2004) 111.
30. F. Bentiss, M. Traisnel, N. Chaibi, B. Mernari, H. Vezin, M. Lagrene’e, *Corros. Sci.* 44 (2002) 2271.
31. L.B. Tang, G.N. Mu, G.H. Liu, *Corros. Sci.* 45 (2003) 2251.
32. G.K.Gomma, M.H.Wahdan, *Mater. Chem. Phys.* 39 (1995) 209.
33. A.Zarrouk, A. Dafali, B. Hammouti, H. Zarrok, S. Boukhris, M. Zertoubi, *Int. J. Electrochem. Soc.*, 5 (2010) 46.
34. R. Arshadi, M. Lashgari, Gh. A. Parsafar, *Mater. Chem. Phys.*, 86 (2004) 311